IMPROVEMENT OF RELATIVE GEOMETRIC CORRECTION FOR MULTIPLE SATELLITE IMAGES BASED ON HOMOGRAPHY BUNDLE ADJUSTMENT

Seunghwan Ban[1], Seunghyeok Choi[2] Taejung Kim*[3]

[1]Graduate Student, [2]Undergraduate Student, *[3]Professor
Department of Geoinformatic Engineering, Inha University
100, Inha-ro, Michuhol-gu, Incheon 22212, Republic of Korea
Email: 22231493@inha.edu, 12181199@inha.edu, tezid@inha.ac.kr

KEY WORDS: Satellite, Image registration, Feature detection, Bundle adjustment

ABSTRACT: Relative geometric correction of satellite images is a technique that adjusts geometric displacements among them based on their relative positional relationships in image space. It has a vital role in improving the overall quality, precision, and reliability of satellite image analysis. With advancements in satellite imaging technology, high-resolution and high-quality images are being collected daily from satellites deployed worldwide. However, in spite of advanced satellite geo-positioning equipment, there are still diverse levels of remaining positional errors. These errors need to be corrected through geometric correction. In case of utilizing more than two satellite images over the same geolocation, performing relative geometric correction among them and an image-to-image registration is still challenging. The challenges lie on selecting rational reference image, or reference plane, on determining image transformation and achieving optimal solution for all image combinations. In this study, we propose a homography-based bundle adjustment for relative geometric correction of multiple satellite images. Our objective is to estimate the optimal reference plane onto which the images are projected and to achieve a fast generation of result images. For experiments, we used multiple high-resolution satellite images from KOMPSAT-3A. The processing level of the used satellite images was L2G, which was processed with precise orthogonal correction. We achieved relative geometric correction of multiple satellite images by the transform estimated by our method. As a result, an initial reprojection error of around 2.52 pixels was corrected to 1.42 pixels. We also confirmed that our proposed method showed more accurate result than a homography-based image-to-image registration method.

1. INTRODUCTION

Recently, the supply of Earth observation satellites is increase and almost all areas of Earth are covered with satellite images every day. These satellite images can be processed into vast time-series data that facilitate analysis such as change detection and land monitoring. Positional errors present in satellite images act as additional error factors for this analysis. Therefore, positional errors must be corrected before utilization. To correct these errors, ground control points (GCPs) and terrain models such as the Digital Elevation Model (DEM) are used for referencing absolute position and removing relief displacements in images. This allows for the alignment of satellite imagery with precise geospatial information (Kim and Im 2003; Son et al., 2021). However, even with geometric and orthorectification corrections applied satellite images may still contain relative geometric errors. Such errors may be significant among images acquired from different satellites and processed separately.

Geometric correction of satellite images is carried out by adjusting the mathematical model inherent in satellite imagery, known as the Rational Function Model (RFM). Relative geometric correction based on RFM also involves treating the extracted tie points as virtual GCPs and estimating the coordinates of these virtual GCPs for image specific RFM adjustments (Song et al., 2021; Tang et al., 2023). This method has an advantage of being able to estimate the optimal 3D positions of adjusted points, thus minimizing misalignment between images. However, it is not suitable for geometrically corrected and orthorectified satellite images due to the substantial time required for generating a virtual terrain model for projection, the need for highly accurate tie points, and the condition of a uniform distribution of extracted tie points. In contrast, the image-to-image registration method, which involves applying transformation models such as homography or affine to align a reference image with another image, is one of the simple techniques for correcting relative geometric correction without GCPs (Zitova and Flusser, 2003; Gong et al., 2022). However, when applying this method to perform relative geometric correction among multiple satellite images, difficulties lie on the selection of an appropriate reference

image or reference plane for image transformation and the achievement of an optimal solution that considers all possible combinations of images.

Bundle adjustment is a technique that simultaneously adjusts all transformation parameters to obtain accurate transformation between image coordinates and ground coordinates in multiple satellite images (Grodecki and Dial, 2003). In this study, we aim to perform rigorous bundle adjustment on multiple satellite images with overlapping areas to correct relative geometric errors. While general satellite image bundle adjustments, including the method by Grodecki and Dial (2003), focus on correcting the RFM equation, our adjustment is performed by reconstructing the adjustment problem as a homography transformation-based bundle adjustment. Our method focuses on offering a faster, more practical approach on selecting the optimal ground reference in contrast to the image-to-image registration method. Our method is performed using automatically extracted tie points as the basis of reference. For tie point extraction, we used the Scale-Invariant Feature Transform (SIFT) algorithm (Lowe, 2004). The extracted tie points were used to form the coefficients of the bundle adjustment observation equations, following an outlier filtering process. Subsequently, bundle adjustment was performed to estimate the homography model for each image.

For the experiments, our input datasets were constructed with multiple high-resolution satellite images acquired from KOMPSAT-3A. Our dataset consisted of four sets of images, each with overlapping areas. These datasets were designed to encompass diverse regions and conditions. To validate the performance of our proposed method, we calculated reprojection errors using manually extracted tie points. We also generated result images by applying the estimated homography model for image transformation that allowed us to visually confirm the relative geometric correction.

2. RELATIVE GEOMETRIC CORRECTION

To apply our relative geometric correction, we need multiple satellite images with overlapping areas and their geo-referencing information as input data. Our method is comprised of four main steps. The first step is tie point extraction, where we improved accuracy and reduced the time required for tie point extraction by utilizing the geo-referencing information of images. The second step involves constructing a matrix with observation equations using the extracted tie points. Image coordinates of the tie points are applied as coefficients in the equations, used to form matrices for bundle adjustments. The third step is homography based bundle adjustment. In this step, we estimate the homography model for image transformation and apply a recursive method to update weights, ensuring a more rigorous approach. The final step is to apply the estimated homography model to perform image transformation. This step is essential for generating visual results to confirm the relative geometric correction and for the practical utilization of satellite images. Figure 1 shows the flowchart of our relative geometric correction process.

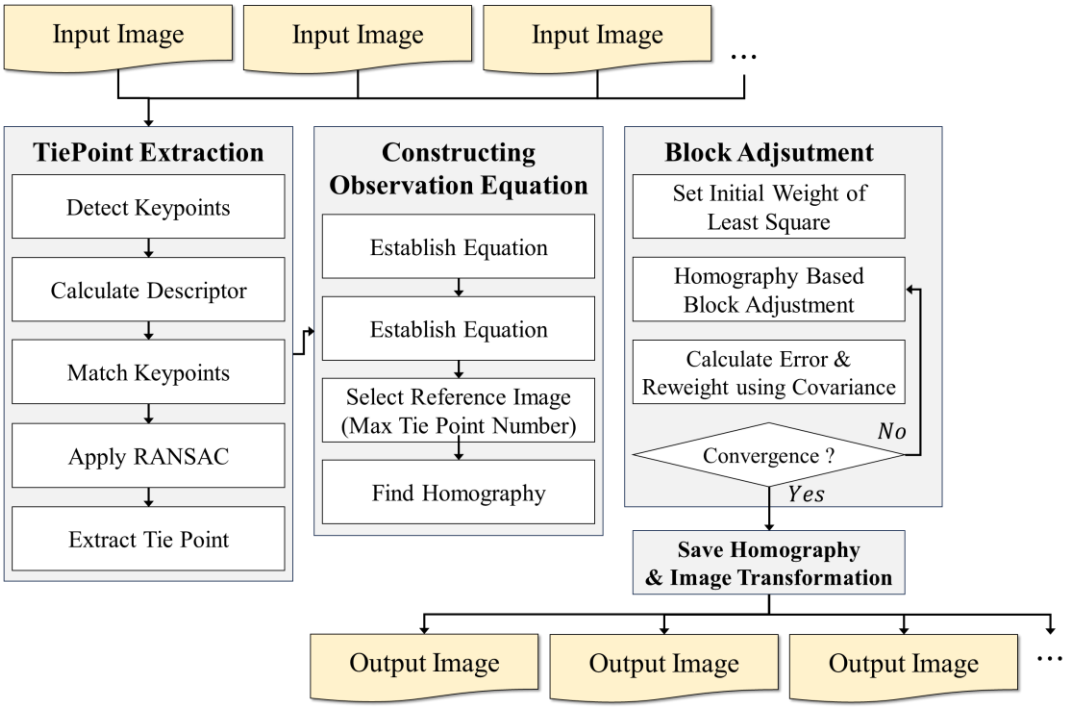

Figure 1. Flow chart of proposed relative geometric correction

2.1 Tie Point Extraction with Overlap Area

We perform tie point matching and filtering that involves identifying corresponding points between the satellite images. For tie point matching, we employed the SIFT algorithm. Since tie point matching is repeated for all image pixels, the processing time also increases as the size of the image increases. Furthermore, the initial matching of tie points is conducted with the closest matching feature points, although a significant number of outliers are present.

To improve the processing speed, we calculate the overlapping area between images to minimize the areas performed for tie point matching. To determine the overlapping areas between images, we utilize the geo-referencing information as relative geometric information. Relative geometric information comprises six elements and includes an affine transformation model for converting between image coordinates and ground coordinates. The conversion equation, presented in Equation (1), allows us to calculate the overlapping area within the ground coordinate system. As shown in Figure 2, we determine the image coordinate corresponding to this overlapping area. Utilizing these calculated image coordinates, we clip the corresponding region in the images. Additionally, to enhance the accuracy of initial tie point matching, we divide the computed overlapping area into nine regions and index the extracted feature points according to the respective region they belonged to. The improved tie point matching assumes that features between the same indices should match because the satellite images used have already been geometrically corrected.

$$X_{geo} = GT_0 + GT_1 \times Column + GT_2 \times Row$$
$$Y_{geo} = GT_3 + GT_4 \times Column + GT_5 \times Row \quad (1)$$

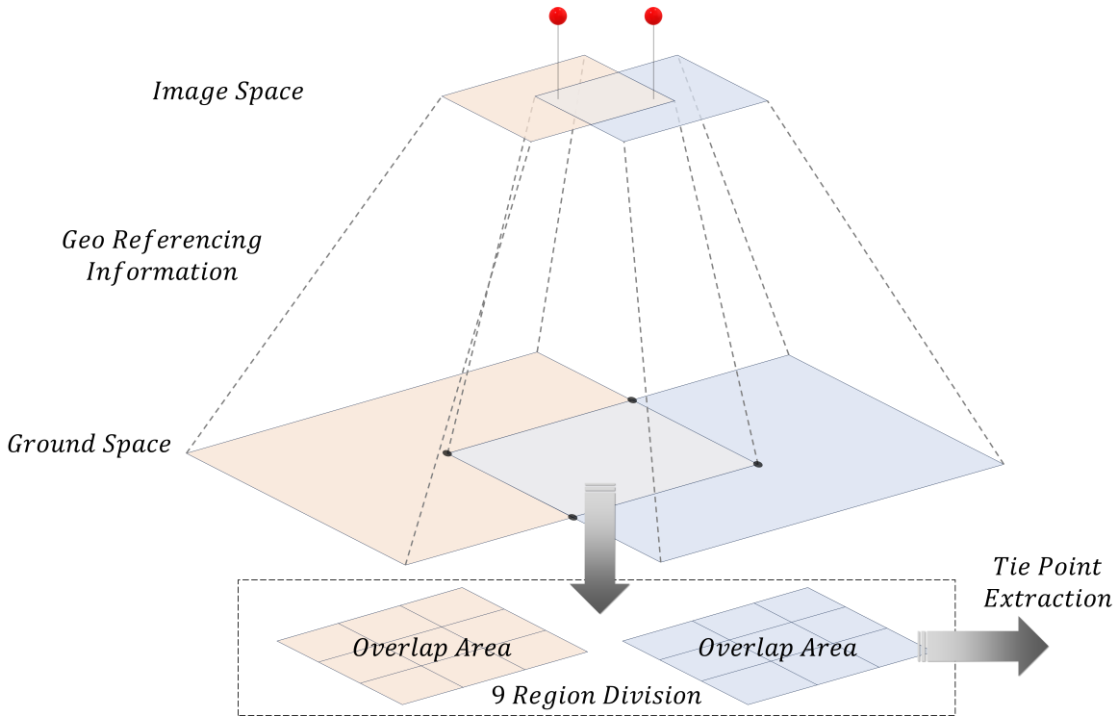

Figure 2. Pre-processing concept for tie point extraction

After initial tie point matching, we apply the Random Sample Consensus (RANSAC) algorithm to filter tie points (Fischler and Bolles, 1981). RANSAC is an iterative robust estimation method used to eliminate outliers in the tie point matching process. In this study, the number of iterations was set to 50,000. We set the threshold for determining outliers to 10 pixels, which allowed for the extraction of a large number of tie points. The combination of our tie point matching process and the RANSAC algorithm enhances the accuracy and robustness of extracted tie points. This allows us to extract high-quality tie points, which serve as dependable references for the subsequent step of the relative geometric correction process.

2.2 Observation Equation and Initialize

Before performing bundle adjustment, we must establish the observation equations using the extracted tie points. Our observation equations are also based on homography, and they are represented by Equation (2). Our equations represent the projection of image coordinates onto ground coordinates using geo-referencing information. Since all images used contain geo-referencing information, the transformation between the image and ground in the form of an affine transformation can be expressed as a homography transformation with the general perspective form (h_8 = 1).

$$\begin{aligned} Column' &= (\, H_0 \cdot Column + H_1 \cdot Row + H_2 \,) \,/\, Denom \\ Row' &= (\, H_3 \cdot Column + H_4 \cdot Row + H_5 \,) \,/\, Denom \\ Denom &= H_6 \cdot Column + H_7 \cdot Row + H_8 \end{aligned} \tag{2}$$

Next, for the estimation of the homography model parameters required for bundle adjustment, it is essential to select rational images focusing on choosing reference images as basis for initializing the homography parameters. We select the reference images with the largest number of extracted tie points as the reference image. As shown in Figure 3, in our method, parameter adjustment takes place within a virtual image space. Consequently, the homography parameters for the reference image are initialized with an identity matrix, and the homography parameters for the remaining images are initialized by estimating the homography transformation model using the image coordinates of the extracted tie points.

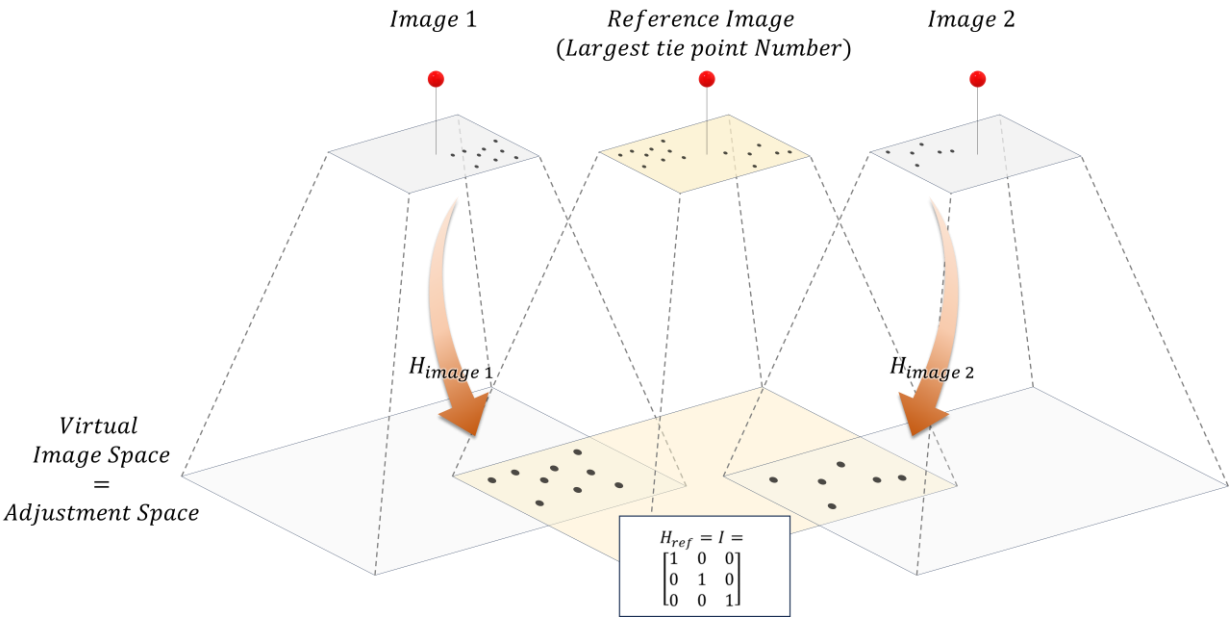

Figure 3. Initializing method of adjustment parameter.

2.3 Homography Based Bundle Adjustment

Bundle adjustment is applied to correct images concurrently and optimize them to achieve precise geometric alignment. In our method, it is applied to multiple satellite images with overlapping areas using the observation equation and tie-points. We propose that handling multiple satellite images is better suited with bundle adjustment-based relative geometric correction method than a pairwise image registration method. A pairwise image registration method often presents difficulties in finding a reference image that accurately represents the entire dataset. Moreover, as the number of images grows the computational demands and time required for pairwise registrations between individual images increase substantially. In contrast, bundle adjustment-based approach excels in handling multiple images concurrently. It optimizes the observation equations using the tie points. As shown in Figure 3, overlapping images define a relative positional relationship between them by utilizing the extracted tie-points, which represent measured image coordinates across those images.

By combining the established observation equations and the concept of adjustment within a virtual image space, our bundle adjustment can be formulated as shown in Equation (3). Extracted tie points are utilized as virtual image coordinates for generating a virtual reference frame. As a result, two observation equations for bundle adjustment can be established for each image coordinates of tie point (i) in image (j) th image with (k) virtual image coordinates in the reference frame.

$$F_{column} = -\ Column_k{}' + \frac{H_0^{(j)} \cdot Column_i + H_1^{(j)} \cdot Row_i + H_2^{(j)}}{H_6^{(j)} \cdot Column_i + H_7^{(j)} \cdot Row_i + H_8^{(j)}}$$
$$F_{row} = -\ Row_k{}' + \frac{H_3^{(j)} \cdot Column_i + H_4^{(j)} \cdot Row_i + H_5^{(j)}}{H_6^{(j)} \cdot Column_i + H_7^{(j)} \cdot Row_i + H_8^{(j)}} \tag{3}$$

By applying Taylor series expansion in Equation (3), it can be expressed as a linearized model using initial value and their increments as shown in Equation (4). In Equation (4), x represents the parameter values that we target to estimate. It signifies the homography transformation parameters for each individual image and the image coordinates for each tie point projected onto the virtual reference frame.

$$F_{i_0} + dF_i + \varepsilon = 0 \tag{4}$$

$$Where,$$

$$F_{i_0} = \begin{bmatrix} F_{column_0} \\ F_{row_0} \end{bmatrix} = \begin{bmatrix} -Column_k' + \dfrac{H_{0_0}^{(j)} \cdot Column_i + H_{1_0}^{(j)} \cdot Row_i + H_{2_0}^{(j)}}{H_{6_0}^{(j)} \cdot Column_i + H_{7_0}^{(j)} \cdot Row_i + H_{8_0}^{(j)}} \\ -Row_k' + \dfrac{H_{0_0}^{(j)} \cdot Column_i + H_{1_0}^{(j)} \cdot Row_i + H_{2_0}^{(j)}}{H_{6_0}^{(j)} \cdot Column_i + H_{7_0}^{(j)} \cdot Row_i + H_{8_0}^{(j)}} \end{bmatrix}$$

$$dF_i = \begin{bmatrix} dF_{column_i} \\ dF_{row_i} \end{bmatrix} = \begin{bmatrix} \dfrac{\partial F_{column_i}}{\partial x} \\ \dfrac{\partial F_{row_i}}{\partial x} \end{bmatrix} dx$$

To estimate the incremental values (dx) of the parameter x, we have reconstructed Equation (4) using a least square approach with initial weights as shown in Equation (5). We have subdivided the parameter increments denoted as dx and corresponding weights into subgroups related to homography and tie points, and represented as Equation (6). The initial weights for homography (W_H) and observation equations (W_E) are initially assigned based on the estimated statistics of the homography, reflecting the precision of the estimated solutions. Additionally, the initial weights for tie points (W_{TP}) are set relatively low to allow for adequate flexible adjustment. In our method, we iteratively estimate the solutions and covariance values for re-weighting to converge toward an accurate relative geometric correction. And M_E, M_H, M_{TP} are misclosures for the observation equations, homography parameter and image coordinates of tie points.

$$W \begin{bmatrix} \dfrac{\partial F_{column_i}}{\partial x} \\ \dfrac{\partial F_{row_i}}{\partial x} \end{bmatrix} dx = W \begin{bmatrix} F_{column_0} \\ F_{row_0} \end{bmatrix} \tag{5}$$

$$\begin{bmatrix} W_E & 0 & 0 \\ 0 & W_H & 0 \\ 0 & 0 & W_{TP} \end{bmatrix} \begin{bmatrix} \dfrac{\partial F}{\partial x_H} & \dfrac{\partial F}{\partial x_{TP}} \\ I & 0 \\ 0 & I \end{bmatrix} \begin{bmatrix} dx_H \\ dx_{TP} \end{bmatrix} = \begin{bmatrix} W_E & 0 & 0 \\ 0 & W_H & 0 \\ 0 & 0 & W_{TP} \end{bmatrix} \begin{bmatrix} M_E \\ M_H \\ M_{TP} \end{bmatrix} \tag{6}$$

For the evaluation of the estimation, the assessment of the estimation result relies on the estimated residuals and the covariance matrix of residuals. The covariance matrix of residuals is determined using Equation (7), following the approach proposed by Mikhail and Ackermann (1976). Furthermore, Equation (8) can be employed to compute the updated weights for subsequent iterations, providing critical insights into the precision and dependability of the estimated parameters. These calculations play a crucial role in evaluating the accuracy of the results and facilitating iterative estimations in subsequent stages of the rigorous bundle adjustment process.

$$C_{vv} = C_{LL} - BC_{\hat{p}\hat{p}}B^T \tag{7}$$

$$Where,$$

$$C_{\hat{p}\hat{p}} = (B^T C_{LL}^{-1} B)^{-1}$$

$$\hat{C}_{LL} = \frac{v^T C_{LL}^{-1} v}{trace(C_{vv} C_{LL}^{-1})} \tag{8}$$

2.4 Image Transformation

To generate the result image demonstrating the relative geometric correction of satellite images, image transformation is achieved by utilizing an image resampling method that relies on the relationship between image coordinates and ground coordinates. While the primary objective of relative geometric correction of satellite images is to rectify the existing pixel errors between images, it is equally crucial to minimize distortion of the original geo-referencing information. However, our bundle adjustment is based on homography transformation which assumes a 2D plane transformation. It operates not by projecting onto ground coordinates using geo-referencing information but rather within a virtual image space where tie points are projected onto a virtual reference frame. This means that the adjusting homography parameters produce results projected at the image level, and the geo-referencing information projected onto the ground for each image is not immediately estimated.

In our approach, we first perform the transformation of the reference image, which is initially used for parameter initialization. Since the initial homography parameters for the reference image are estimated starting from an identity matrix, the final estimated homography parameters can be combined with the original geo-referencing information of the reference image to estimate new geo-referencing information. Figure 4 demonstrates the concept of our image transformation method. The final estimated homography parameter can be applied to the original image, enabling the execution of homography transformation. As shown in the transformed homography result in Figure 4, the application of the homography results in the computation of the coordinates of the top-left and bottom-right corners including any blank space. This information is used to determine the position at which the result image will be generated and to calculate the pixel count.

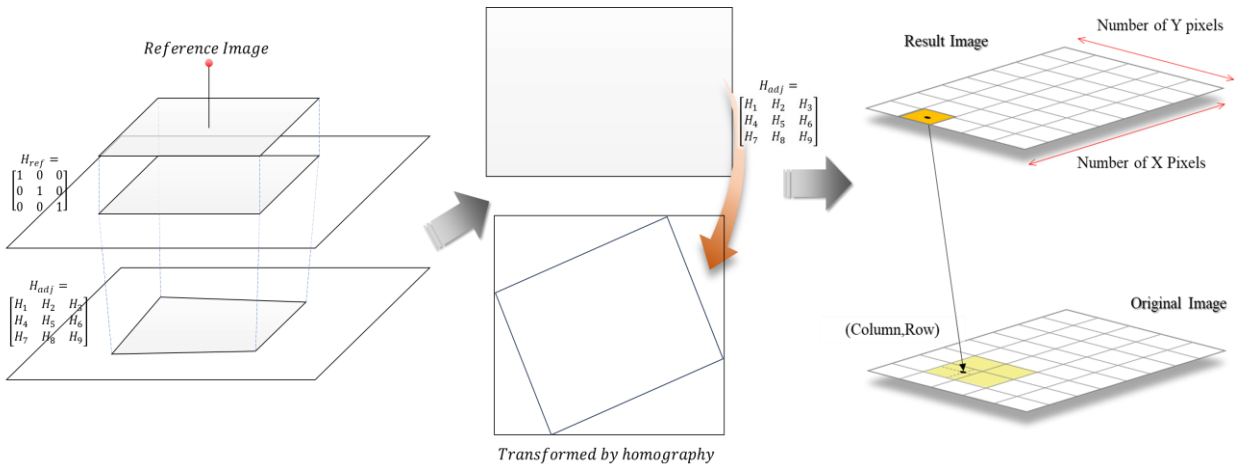

Figure 4. Image transformation method.

The generation of the result image involves applying a resampling method that uses the inverse of the homography model through a technique known as the inverse projection resampling method. The inverse projection resampling method applies pre-calculating size and position of the result images, and extracting pixel values from the original image for each corresponding pixel. The pixel position can be easily calculated using the inverse of the homography model. When computing pixel values, as the projected pixel coordinates in the original image do not always align with the center of the pixels, interpolation methods are employed. In our study, we used bilinear interpolation to perform this operation. Finally, the result image is equipped with its original geo-referencing information. As mentioned in Chapter 2.1, the geo-referencing information describes the transformation relationship between the image and the ground in the form of an Affine transformation. When applied to the result image, it takes into account the coordinates of the top-left corner, the ground sample distance (GSD) in the row and column directions, as well as any rotation. The remaining images, excluding the reference image, are also used to project onto the reference frame using homography parameters to create the result image. One difference is that during the final coordinate assignment step, the geo-referencing information from the reference image is used to prevent pixel boundary mismatches with the reference image. This approach is particularly suitable for our datasets consisting of the same satellite imagery, such as KOMPSAT-3A.

3. EXPERIMENTS

For the experiments, we constructed the test datasets using multiple high-resolution satellite images acquired from the KOMPSAT-3A satellite. The experiments were conducted using a total of four datasets. Two of these datasets consisted of two images each. They were designed for comparing the differences between the proposed method and image-to-image registration. The remaining two datasets were constructed to assess the applicability of the approach to multiple satellite images. All datasets were designed to include overlapping areas to facilitate tie point extraction for relative geometric correction. The images were carefully selected to cover various geographical regions and environmental conditions. Figure 5 shows the positions, areas, and overlapping relationships of the datasets used in our experiments. The right side of each dataset in Figure 5 shows enlarged images by color compositing of images constituting the dataset. As shown in the enlarged images, there were mismatches of the same object due to relative positional errors between satellite images. All satellite images used in the experiments were Level 2G, which processed geometric correction and orthorectification and contained geo-referencing information.

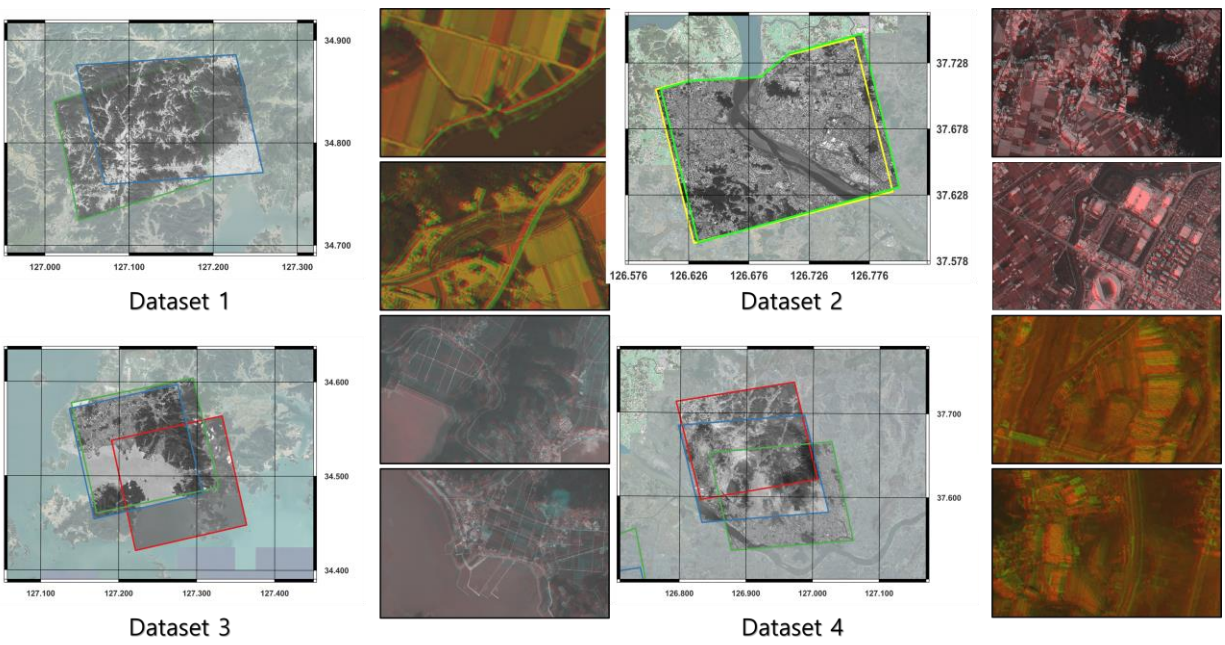

Figure 5. Location and initial position errors of used datasets.

Table 1 shows the attributes of the KOMPSAT-3A satellite image dataset used in these experiments. For datasets consisting of three images (dataset 3 and 4), the initial relative errors were calculated based on the re-projection errors between image excluding the reference image. It is worth noting that relative positional errors existed even though the satellite images used had undergone geometric and orthorectification corrections.

Table 1. Information of used dataset.

Dataset Number	Date of Acquisition	Image Center Latitude	Image Center Longitude	Tie Point Number	Initial Relative Error
1	2017. 10. 21	34.7687992 °	127.1469898 °	6,351	4.18 pixels
	2017. 11. 09	34.7960765 °	127.2295844 °		
2	2018. 01. 19	37.4461607 °	126.6744010 °	4,867	2.43 pixels
	2018. 01. 27	37.4798140 °	126.6632889 °		
3	2016. 04. 15	34.5260062 °	127.2219351 °	2,292	4.378 pixels
	2016. 08. 19	34.4927072 °	127.2772040 °		
	2016. 12. 31	34.5326569 °	127.2336473 °		
4	2016. 01. 08	37.6009283 °	126.9528703 °	13,355	13.059 pixels
	2017. 02. 15	37.6339461 °	126.9106899 °		
	2017. 02. 24	37.6678493 °	126.9014737 °		

As shown in Table 1, we performed bundle adjustment using only tie points for the four datasets. To validate the performance of our proposed method, we extracted check points manually for each dataset. For our relative geometric correction, these check points were identified visually as corresponding points on the images, rather than being based on actual ground coordinates. The extracted check points were utilized to calculate the re-projection error using estimated homography parameters. To calculate this error, we projected the image coordinates onto the virtual image spaces using a homography model and re-projected the projected ground coordinates onto the other images.

Table 2 presents the experiment results. All the errors represented in the experiment results refer to re-projection errors, which could be categorized into two groups: model errors and check point errors, as shown in Table2. Model errors quantify how well the extracted tie-points adhere to the estimated homography model based on those tie-points. Check point errors represents the re-projection errors of manually extracted check points. Since these errors are not influenced to the model estimation, the accuracy of check points serves as the most reliable indicator of a practicality.

Dataset Number	Tie Point Number	Initial Relative Error	2D homography		Homography Block Adjustment	
			Model Error	Check Error	Model Error	Check Error
1	6,351	4.18 pixels	1.12 pixels	1.22 pixels	0.56 pixels	1.24 pixels
2	4,867	2.43 pixels	1.13 pixels	1.39 pixels	0.57 pixels	1.40 pixels
3	2,292	4.38 pixels	**Reference**	(1,2) 1.08 pixels (1,3) 1.16 pixels (2,3) 4.38 pixels	0.56 pixels	(1,2) 1.44 pixels (1,3) 1.12 pixels (2,3) 1.60 pixels
			1.08 pixels		0.69 pixels	
			1.16 pixels		0.57 pixels	
4	13,355	13.06 pixels	**Reference**	(1,2) 0.90 pixels (1,3) 2.03 pixels (2,3) 1.89 pixels	0.53 pixels	(1,2) 0.96 pixels (1,3) 1.79 pixels (2,3) 1.64 pixels
			1.79 pixels		0.56 pixels	
			3.26 pixels		0.75 pixels	

In the dataset 1 and dataset 2 consisting of two images, the result of the proposed showed a lower model error which a higher level of compared to 2D homography transformation method. The check point errors showed slightly higher for the proposed method compared to the 2D homography transformation. However, the differences could be considered negligible and nearly equivalent. This merit was accredited to our proposed method; it enabled equally distributed errors across all images by estimating new reference frame without assuming a fixed reference like 2D homography transformation. This result became even more presented in the experiments with dataset 3 and 4. In this case, the accuracy of check points relative to the fixed reference image was precisely estimated. However, for the re-projection errors between the images excluding the reference image, they exhibited significant discrepancies. In contrast, the check point errors in our proposed method were evenly distributed across all images. This merit was also accredited to our proposed method; it corrected relative positional errors considering all the images collectively.

Figure 6 shows the original satellite images before performing relative geometric correction and the result images generated using our proposed method. The original images in Figure 6 shows noticeable relative positional errors between images, as indicated in Table 1 with the relative errors. It leads to the observed discrepancies in the same objects. To verify the effectiveness of the initial error correction, we enlarged the result images for each dataset and conducted a visual comparison of the objects identified in these images. The proposed method successfully mitigated the relative positional errors. These enhancements are visually evident in Figure 6, where could observed the substantial improvements in object alignment and the notable reduction in positional discrepancies across tie image.

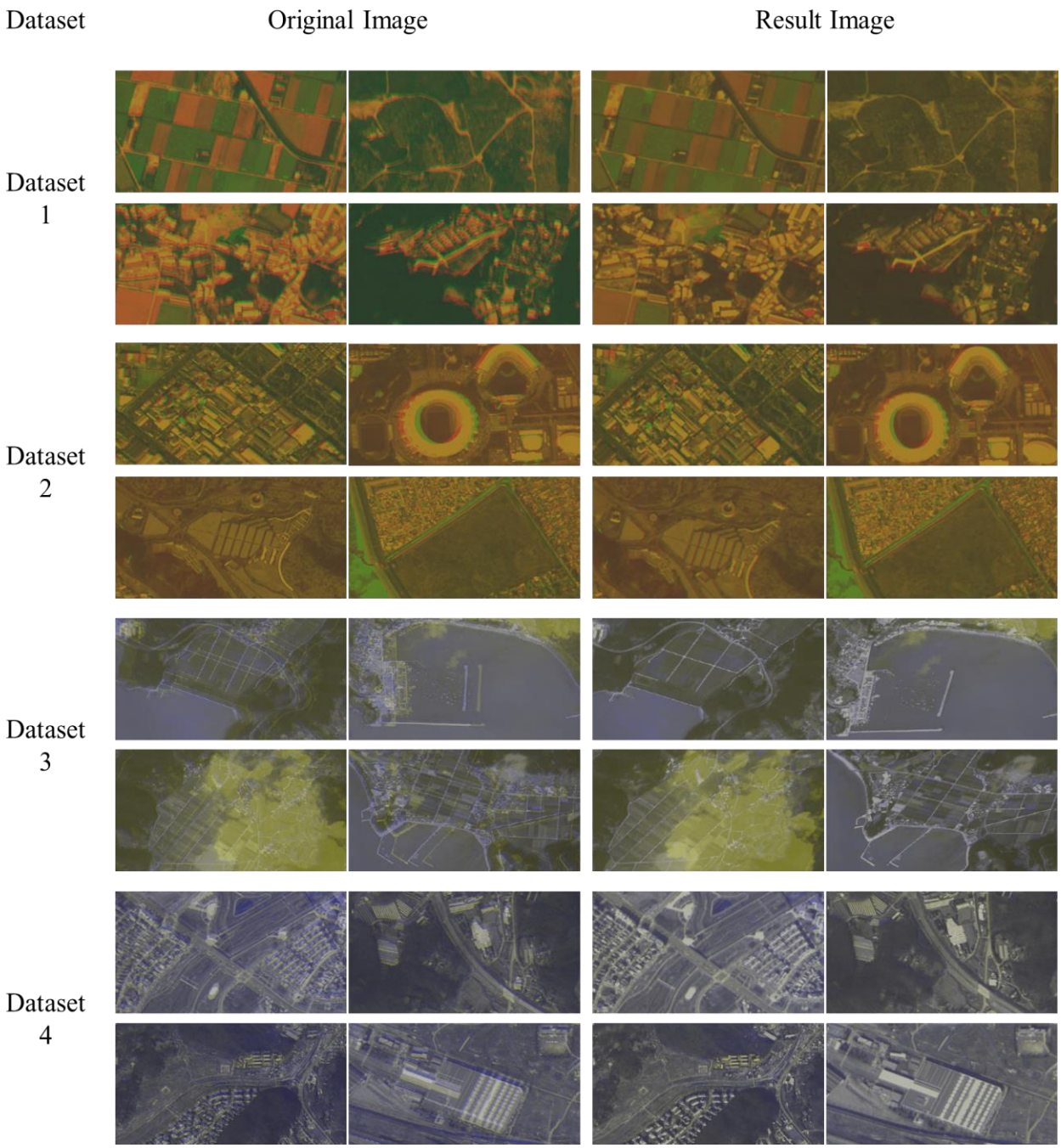

Figure 6. Result image with our relative geometric correction method.

4. CONCLUSIONS

This paper proposed a novel method designed to address the challenges of relative geometric correction for multiple satellite images. Our proposed method for relative geometric correction utilized tie points without need for GCPs. It applied a bundle adjustment approach based on the homography transformation model. It also used the geo-referencing information inherent in satellite images to enhance tie point extraction performance and to reduce processing time. Homography based bundle adjustment outperformed and overcame limitations of image-to-image registration method. Experiments results using KOMPSAT-3A images with a 0.5m ground sampling distances demonstrated an average relative positional error of 1.43 pixels. Visual demonstration sowed improved alignments with enhanced reliability and accuracy was achieved. In conclusion, the bundle adjustment with recursive approach could stand as a robust and efficient solution for relative geometric correction in multiple satellite images. By employing tie points and homography model, our method effectively rectified initial position errors and enhanced the overall accuracy and alignment between images. This research would contribute significantly to the advancement of satellite image processing, providing more accurate and reliable opportunities for Earth observation data.

ACKNOWLEDGEMENT

This work is supported by the Korea Agency for Infrastructure Technology Advancement (KAIA) grant funded by the Ministry of Land, Infrastructure and Transport (Grans RS-2022-00155763)

REFERENCES

Fischler, M. A. and Bolles, R. C., 1981. Random sample consensus: a paradigm for model fitting with applications to image analysis and automated cartography. *Communications of the ACM*, 24(6). pp. 381-395.

Gong, X., Yao, F., Ma, J., Jiang, J., Lu, T., Zhang, Y and Zhou, H., 2022. Feature matching for remote-sensing image registration via neighborhood topological and affine consistency. *Remote Sensing*, 14(11). pp. 2606.

Grodecki, J. and Dial, G., 2003. Block adjustment of high-resolution satellite images described by rational polynomials. *Photogrammetric Engineering & Remote Sensing*, 69(1). pp. 59-68.

Kim, T. and Im, Y. J., 2003. Automatic satellite image registration by combination of matching and random sample consensus. *IEEE transactions on geoscience and remote sensing*, 41(5). pp. 1111-1117.

Loew, D. G., 2004. Distinctive image features from scale-invariant keypoints. *International Journal of Computer Vision*, 60. pp. 91-110.

Son, J. H., Yoon, W., Kim, T. and Rhee, S., 2021. Iterative Precision Geometric Correction for High-Resolution Satellite Images. *Korean Journal of Remote Sensing*, 37(3), pp. 431-447.

Song, W., Liu, S., Tong, X., Niu, C., Ye, Z. and Jin, Y., 2021. Combined geometric positioning and performance analysis of multi-resolution optical imageries from satellite and aerial platforms based on weighted RFM bundle adjustment. *Remote Sensing*, 13(4). pp. 620.

Tang, X., Zhu, X., Hu, W. and Ding, J., 2023. Geometric accuracy analysis of regional block adjustment using GF-7 stereo images without GCPs. *Remote Sensing*, 15(10). pp. 2552.

Zitova, B. and Flusser, J., 2003. Image registration methods: a survey. *Image and Vision Computing*, 21(11). pp. 977-1000.